DIRBE Minus 2MASS: Confirming the Cosmic Infrared Background at 2.2 Microns

Edward L. Wright

Department of Physics and Astronomy, University of California, Los Angeles, CA 90095-1562

wright@astro.ucla.edu

ABSTRACT

Stellar fluxes from the 2MASS catalog are used to remove the contribution due to Galactic stars from the intensity measured by DIRBE in four regions in the North and South Galactic polar caps. After subtracting the interplanetary and Galactic foregrounds, a consistent residual intensity of 14.8 ± 4.6 kJy sr^{-1} or 20.2 ± 6.3 nW m^{-2} sr^{-1} at 2.2 μm is found. At 1.25 μm the residuals show more scatter and are a much smaller fraction of the foreground, leading to a weak limit on the CIRB of 12.0 ± 6.8 kJy sr^{-1} or 28.9 ± 16.3 nW m^{-2} sr^{-1} (1 σ).

Subject headings: cosmology: observations — diffuse radiation — infrared:general

1. Introduction

The Diffuse InfraRed Background Experiment (DIRBE) on the COsmic Background Explorer (*COBE*, see Boggess *et al.* (1992)) observed the entire sky in 10 infrared wavelengths from 1.25 to 240 μm. Hauser *et al.* (1998) discuss the determination of the Cosmic InfraRed Background (CIRB) by removing foreground emission from the DIRBE data. This paper detected the CIRB at 140 and 240 μm, but only gives upper limits at shorter wavelengths. From 5 to 100 μm, the zodiacal light foreground due to thermal emission from interplanetary dust grains is so large that no reliable estimates of the CIRB can be made from a position 1 AU from the Sun (Kelsall *et al.* 1998). In the shorter wavelengths from 1.25 to 3.5 μm, the zodiacal light is fainter, but uncertainties in modeling the foreground due to Galactic stars are too large to allow a determination of the CIRB (Arendt *et al.* 1998). Recently, Gorjian *et al.* (2000) removed the Galactic star foreground by directly measuring the stars in a $2^\circ \times 2^\circ$ box using ground-based telescopes and then subtracting the stellar contribution from the DIRBE intensity on a pixel-by-pixel basis. This field, a DIRBE dark spot, was selected using DIRBE data to have a minimal number of bright Galactic stars. In addition, Wright & Reese (2000) used a histogram fitting method to remove the stellar foreground from the DIRBE data in a less model-dependent way than that used by Arendt *et al.* (1998). Gorjian *et al.* (2000) and Wright & Reese (2000) obtained consistent estimates of the CIRB at 2.2 and 3.5 μm. With the recent 2^{nd} incremental release of 2MASS data, it is now possible to apply the direct subtraction method of Gorjian *et al.* (2000) to four additional DIRBE dark spots scattered around the North and South Galactic polar caps.

Kashlinsky & Odenwald (2000) have claimed a detection of the fluctuations of the CIRB. Kashlinsky & Odenwald (2000) also give the range 0.05 to 0.1 for the ratio of the fluctuations in the DIRBE beam to the mean intensity for the CIRB. But this ratio and fluctuation combine to give a range of CIRB values that is incompatible with the Hauser *et al.* (1998) upper limits on the CIRB, especially at 1.25 μm. Furthermore, the claimed cosmic fluctuations are larger than the residuals in the DIRBE−2MASS fits presented in §3. In this paper, Kashlinsky & Odenwald (2000) is treated as an upper limit on the CIRB which is compatible with previous limits and the results found here. Wright (2001) will discuss the possible cosmic fluctuation signal in the DIRBE−2MASS residuals in more detail.

2. Data Sets

The two main datasets used in this paper are the DIRBE maps and the 2MASS point source catalog (PSC).

The DIRBE weekly maps were used: DIRBE_WKnn_P3B.FITS for $04 \leq \mathrm{nn} \leq 44$. These data and the very strong no-zodi principle described by Wright (1997) were used to derive a model for the interplanetary dust foreground that is described in Wright (1998) and Gorjian *et al.* (2000). The zodiacal light model was then subtracted from each weekly map, and the remainders were averaged into mission averaged, zodiacal subtracted maps. At 1.25 and 2.2 μm, no correction for interstellar dust emission is needed (Arendt *et al.* 1998). The pixels in these mission averaged, zodiacal subtracted maps provide the DIRBE data, D_i.

DIRBE has a $0.7^\circ \times 0.7^\circ$ square beam with a diagonal of 1°. Thus a thick buffer ring is needed around any studied field to keep bright stars outside the field from influencing the measured DIRBE intensity. One can minimize the resulting inefficiency by studying fields with a large area:perimeter ratio. Large circular regions have the largest area:perimeter ratio, and for circles as large as 3° diameter it is still possible to find fields that have no stars brighter than the 2MASS saturation limit. To find such fields, a list of DIRBE dark spots was generated by smoothing the zodi-subtracted 3.5 μm map with a kernel given by

$$\log_2 W = \frac{-|\hat{n} - \hat{n}'|^2}{3(0.03023^2 - |\hat{n} - \hat{n}'|^2)} \tag{1}$$

where $\hat{n}$ and $\hat{n}'$ are unit vectors. This kernel and all of its derivatives are continuous, and it vanishes identically for radii greater than $2\sin^{-1}(0.03023/2) = 1.732^\circ$. The FWHM is 3°. The 20 faintest spots of the smoothed map in the Northern Galactic Hemisphere and the 20 faintest spots in the Southern Galactic Hemisphere were then located. The darkest spot is in the Northern Hemisphere and was studied by Gorjian *et al.* (2000) using ground-based data.

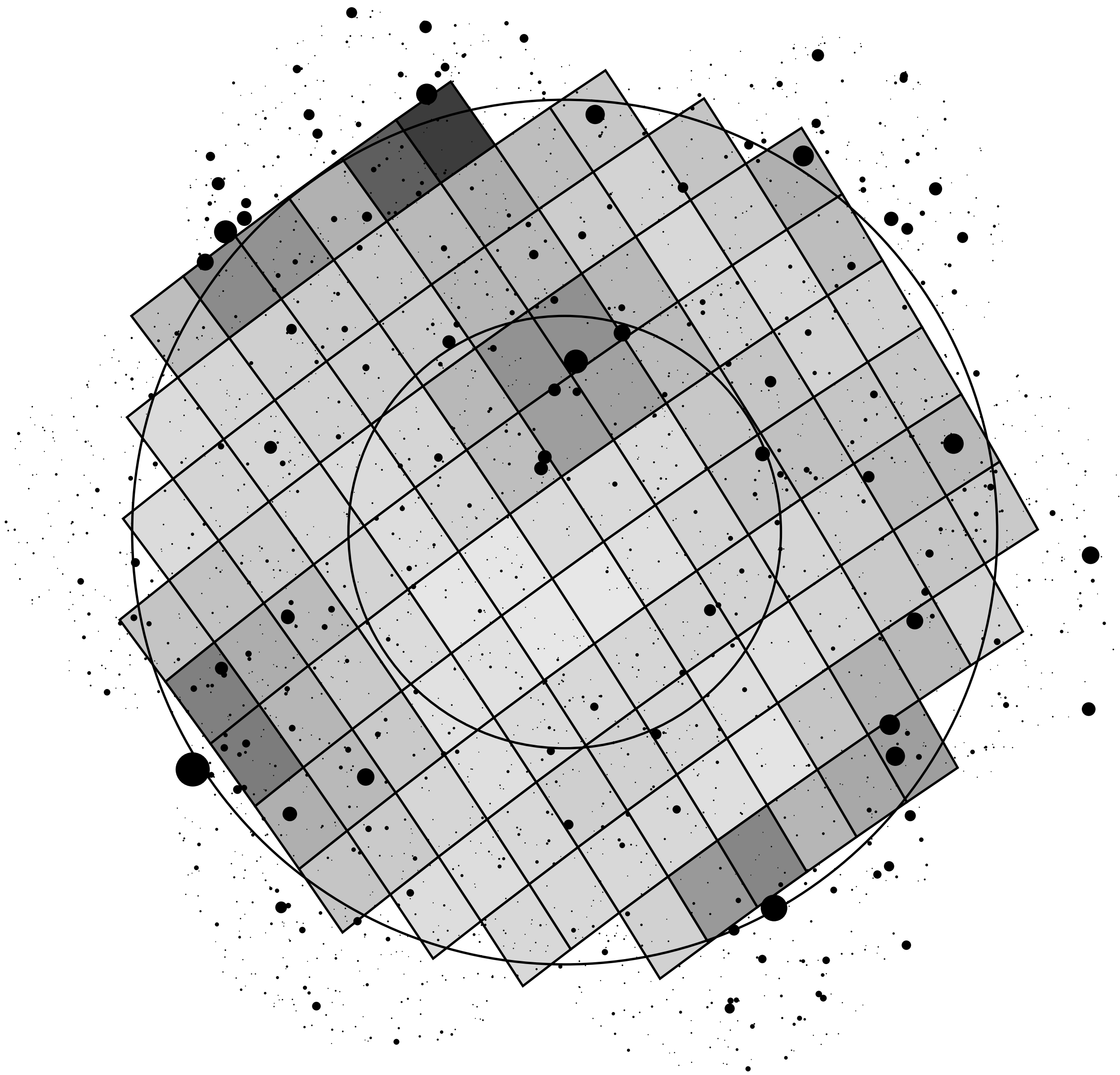

Fig. 1.— The field near the dark spot at $(l, b) = (107.7°, 57.7°)$. The grid shows the DIRBE pixel outlines, while the grayscale indicates the DIRBE flux at 2.2 μm. The filled black circles are the 2MASS stars with $K_s < 12.5$, with the circle area proportional to the flux. The large open circles show a 1 and 2° radius around the dark spot.

The 2MASS data were obtained over the WWW between 16 Mar 2000 and 23 Mar 2000. The IRSA interface was used to search the catalog. This allows a maximum search area of a 1° radius circle, which is too small for a comparison to the DIRBE data taken with a 0.7° beam. Therefore, a total of seven cone searches in a pattern consisting of a hexagon plus the central position were made around each DIRBE dark spot. These searches were restricted to stars brighter than $K_s = 14$. The seven resulting files were combined by stripping the table headers, concatenating, sorting, and then using the UNIX uniq filter. If there are no gaps in the 2MASS coverage near a dark spot, this yields a catalog that covers a 2° radius circle around the dark spot plus six small "ears." Only stars within the circle were used in this analysis. However, there are usually gaps in the 2MASS coverage. Searching the 20 darkest spots in each of the Galactic polar caps produced only four usable fields out of 40 candidates. These are listed in Table 1. β is the ecliptic latitude. The combined catalogs for each field were converted into star charts which were checked for missing 2MASS data. Two of these four fields have coverage gaps near the edge of the 2° radius circle, and thus have $r < 2°$ and a smaller but still useful number of pixels. Figure 1 shows the 2MASS catalog stars superimposed on the DIRBE map for the dark spot at $(l, b) = (107.7°, 57.7°)$.

3. Analysis

The DIRBE data for the i^{th} pixel is D_i, and should be the sum of the zodiacal light, Z_i; the cataloged stars, B_i; the faint stars, F_i; and the CIRB, C. The cataloged star contribution is found using the method of Gorjian *et al.* (2000) on all stars brighter than $K = 14$. In this method, the DIRBE beam center is assumed to be uniformly distributed within the area of the i^{th} pixel, and the DIRBE beam orientation is assumed to be uniformly distributed in position angle. Under these assumptions, the probability that the j^{th} star contributes to the signal in the i^{th} pixel is p_{ij}, and the cataloged star contribution is

$$B_i = \Omega_b^{-1} \sum_j p_{ij} S_j \tag{2}$$

where S_j is the flux of the j^{th} star and Ω_b is the solid angle of the DIRBE beam.[1] Figure 2 shows the probability p_{ij} for stars located in the center, near an edge, or near a corner of a pixel located near the center, an edge, or a corner of a cube face in the quadrilateralized spherical cube pixel scheme. The standard deviation of the bright star contribution is given by

$$\sigma^2(B_i) = \Omega_b^{-2} \sum_j [p_{ij}(1 - p_{ij}) + p_{ij}^2(0.1 + (0.4 \ln 10)^2 \sigma^2(m_j))] S_j^2. \tag{3}$$

The first term in the []'s in Equation 3 is the "flicker noise" caused by a star that is on the edge of the DIRBE beam. The second term represents the flux error for the j^{th} star, and it includes a

[1]Gorjian *et al.* (2000) used Ω_p instead of Ω_b in Equation 2: this is appropriate for p's normalized to the total flux as in Table 5 of Wright & Reese (2000), but for p's normalized to a peak of unity as in Figure 2 the beam solid angle must be used for the normalization of Equation 2.

generous allowance for variability between the time of the DIRBE observations and the the time of the 2MASS observations: the "0.1" corresponds to $\sigma = 0.34$ magnitudes. This standard deviation is shown by the error bars in Figures 3 and 4. The actual noise on the DIRBE data is negligible: 1 kJy sr^{-1} at 1.25 μm and 1.2 kJy sr^{-1} at 2.2 μm (Hauser *et al.* 1998). The uncertainty in the DIRBE zero level, or offset, is also negligible (Hauser *et al.* 1998). The CIRB should be isotropic, and F should vary only slightly within a 2° radius of a dark spot. But both the zodi-subtracted data, DZ$_i$, and the bright star contribution fluctuate greatly from DIRBE beam to DIRBE beam due to the confusion noise caused by overlapping stars. Figures 3 and 4 show plots of DZ$_i$ *vs.* B_i for each of the four fields. The gray points with large error bars are pixels with a bright star at the edge of the beam. These bright stars usually saturate the 2MASS survey, and are assigned a nominal magnitude of 4 and a nominal flux error of a factor of ten. This large flux error guarantees that the pixels affected by saturated stars have no effect on the subsequent analysis. The lines have unit slope with intercepts determined using a weighted median procedure. The average values of the data D$_i$, the zodi-subtracted data DZ$_i$, and the derived intercepts DZ(0) for each of the four fields are given in Table 1.

The 2MASS K_s magnitudes were converted to DIRBE fluxes using the $F_\circ(K) = 614$ Jy derived by Gorjian *et al.* (2000) from the median of determinations using seven bright red stars. This assumes that there is no significant $K_s - K$ color difference between the red calibration stars used by Gorjian *et al.* (2000) and the stars in the dark spots. The 2MASS observations saturate [even in the first read] on stars brighter than 5^{th} magnitude. At this level, the DIRBE data are still substantially affected by confusion noise, so a direct comparison of DIRBE and 2MASS on the same stars will not give a high precision result, but the overall agreement between the unity slope lines and the data in Figures 3 and 4 shows that a direct DIRBE to 2MASS comparison is consistent with the Gorjian *et al.* (2000) calibration. Figure 5 shows a histogram of the values DZ$_i - B_i -$ DZ(0) for the four dark spots combined. Note that the standard deviations derived from the three highest bins of these histograms of the individual histograms are 1.27, 1.93, 2.82, and 2.93 kJy sr^{-1}, while the standard deviation of the Gaussian fit in Figure 5 is 1.81 kJy sr^{-1}. Since this histogram includes the DIRBE detector noise, any small scale errors in the zodiacal light model, any small scale structure in the faint star contribution, a contribution from stellar variability, and a calibration error contribution in addition to any real extragalactic fluctuation, one can take 1.81 kJy sr^{-1} = 2.47 nW m^{-2} sr^{-1} as an upper limit on the extragalactic fluctuation δC_{rms}.

Stars fainter than $K = 14$ contribute a small amount which must be subtracted from the intercepts. This contribution was evaluated using the Wainscoat *et al.* (1992) star count model. But Wright & Reese (2000) and Gorjian *et al.* (2000) find that this model overpredicts high latitude star counts by 10% in the $6 < K < 12$ range. After applying this 10% correction, which assumes that the same ratio applies to $K > 14$, the faint star corrections are F = 1.58, 1.87, 1.50, and 2.03 kJy sr^{-1} in the four fields. An uncertainty of 10% of the total model prediction is assigned to this correction, and listed in Table 2 under "Faint Source". Galaxies brighter than

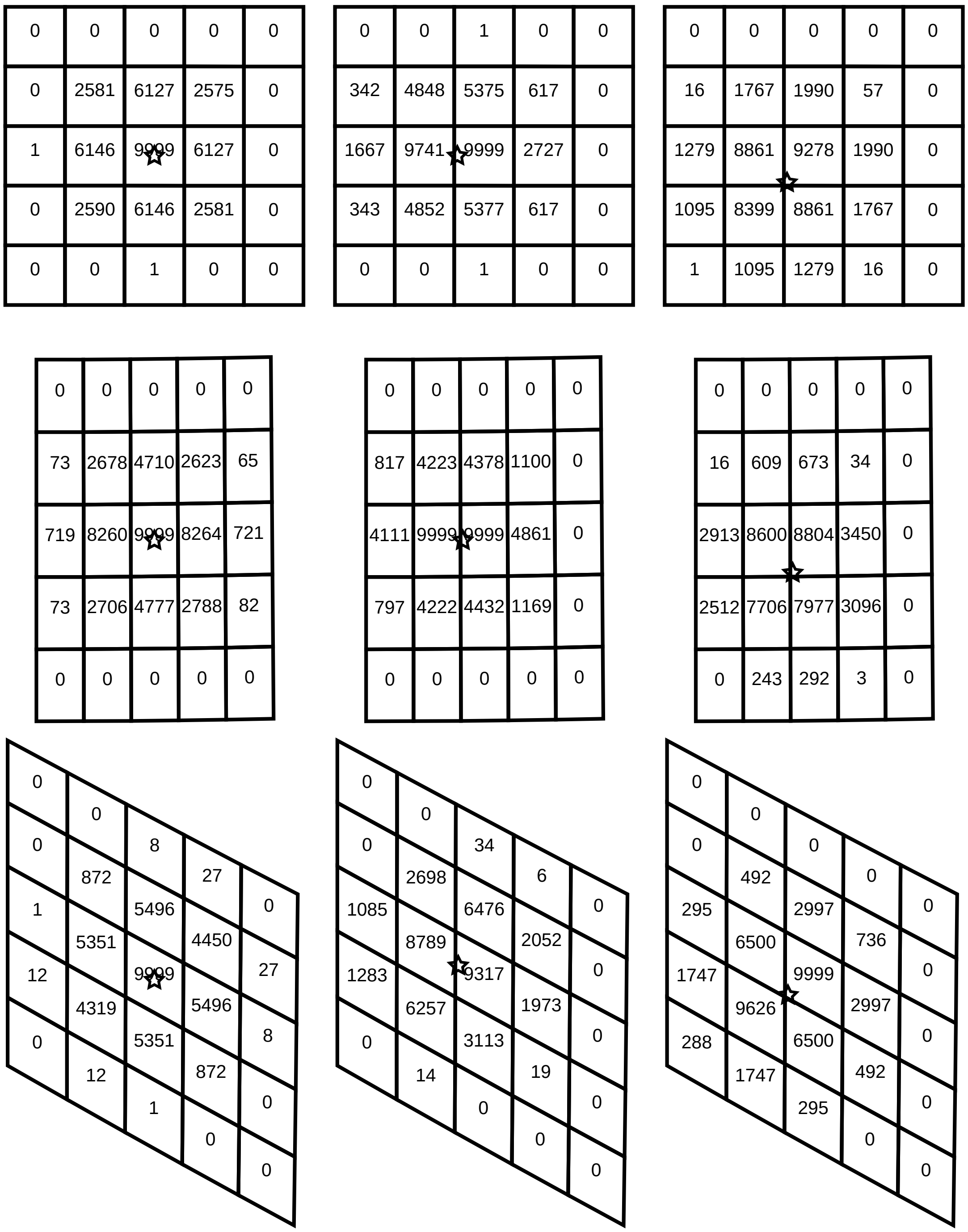

Fig. 2.— The probability of a star at various locations within the DIRBE pixel grid contributing to the signal in various pixels. The top row is near the center of a cube face, the middle row is near an edge of a cube face, and the bottom row is near a corner of a cube face. The numbers within each pixel are $9999p_{ij}$.

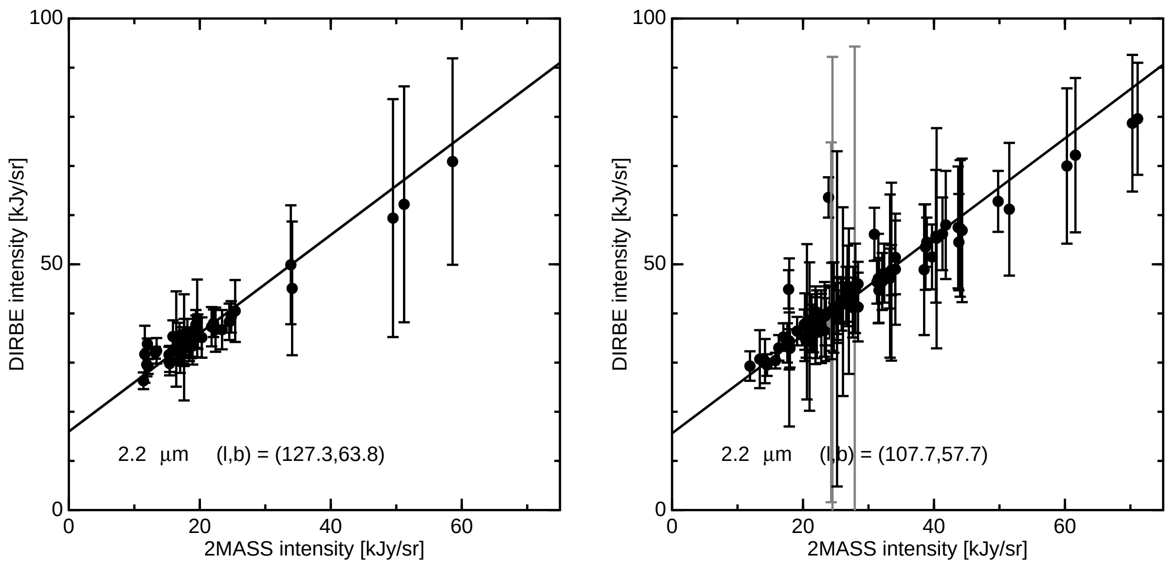

Fig. 3.— Correlations of the DIRBE intensities *vs.* intensities computed from 2MASS fluxes in two Northern DIRBE dark spots.

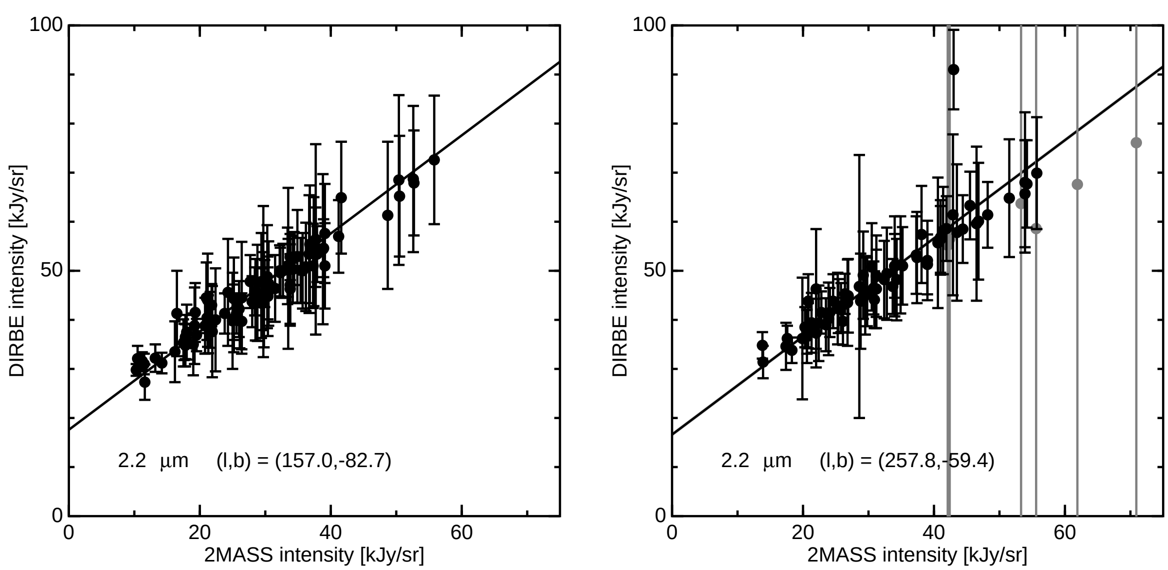

Fig. 4.— Correlations of the DIRBE intensities *vs.* intensities computed from 2MASS fluxes in two Southern DIRBE dark spots.

l [°]	b [°]	β [°]	r [°]	N_{pix}	$\langle D_i \rangle$ [kJy/sr]	$\langle DZ_i \rangle$ [kJy/sr]	DZ(0) [kJy/sr]	CIRB [kJy/sr]
127.3	63.8	50.8	1.5	44	139.65	36.77	15.98	14.50
107.7	57.7	61.0	2.0	86	138.85	44.61	15.62	13.85
157.0	-82.7	-26.0	2.0	86	214.58	46.22	17.60	16.20
257.8	-59.4	-57.9	1.9	78	157.73	52.78	16.62	14.69

Table 1: Locations, sizes and intensities of the 4 DIRBE dark spots at 2.2 μm.

$K = 14$ may be subtracted incorrectly, and their contribution should be added back into the CIRB. Galaxies with $K < 14$ add up to 0.35 kJy sr^{-1}, according to the empirical fits of Gardner *et al.* (1993). A fraction of these galaxies will be in the 2MASS PSC and, since galaxies should not be subtracted, these incorrectly subtracted galaxies should be added back to the CIRB. The fluxes in the 2MASS Extended Source Catalog objects with $K_s < 14$ add up to 0.25 kJy sr^{-1}, indicating that the correction for galaxies in the PSC should be on the order of 0.1 kJy sr^{-1}. In addition, 30% of the Extended Source Catalog objects are coincident with PSC objects suggesting that the compact galactic nuclei – which are in the PSC but should not be subtracted from the CIRB – account for 0.1 kJy sr^{-1}. Thus the CIRB estimates shown in Table 1 are given by $\mathrm{DZ}(0) - \mathrm{F} + 0.1$ kJy sr^{-1}. An uncertainty of 100% of this correction is included in Table 2 under "Galaxies".

Note that the statistical uncertainties in the intercepts are all ≤ 0.4 kJy sr^{-1} and thus negligible compared to systematic errors in the interplanetary dust model. Gorjian *et al.* (2000) adopt an uncertainty of 5% of the zodiacal intensity at the ecliptic poles, and this gives an uncertainty of ± 3.79 kJy sr^{-1}. The effect of a ± 10% calibration error between the DIRBE flux scale and the 2MASS magnitude scale would be a systematic ± 2.58 kJy sr^{-1} change in the CIRB. The precision of the Gorjian *et al.* (2000) calibration of the DIRBE K-band fluxes to the standard infrared magnitude is ± 2.1%. This DIRBE flux calibration agreed with Arendt *et al.* (1998) calibration to better than 1%. Thus a 10% uncertainty in the DIRBE *vs.* 2MASS calibration appears to be conservative. This uncertainty is listed in Table 2 under "Calibration". The mean of the CIRB estimates in Table 1 is 14.79 ± 0.51 kJy sr^{-1}. This standard deviation of the mean of the 4 fields is listed in Table 2 under "Scatter". Finally, the largest uncertainty is the zodiacal light modeling uncertainty. Adding the errors in Table 2 in quadrature gives a result of 14.8 ± 4.6 kJy sr^{-1} or 20.2 ± 6.3 nW m^{-2} sr^{-1}.

4. J Band

For the J-band the contribution from stars with $J < 14$ *and* $K < 14$ was calculated on a pixel by pixel basis. This dual wavelength magnitude selection is essentially equivalent to a simple $J < 14$ selection. There are very few stars in high Galactic latitude fields with color $J - K < 0$.

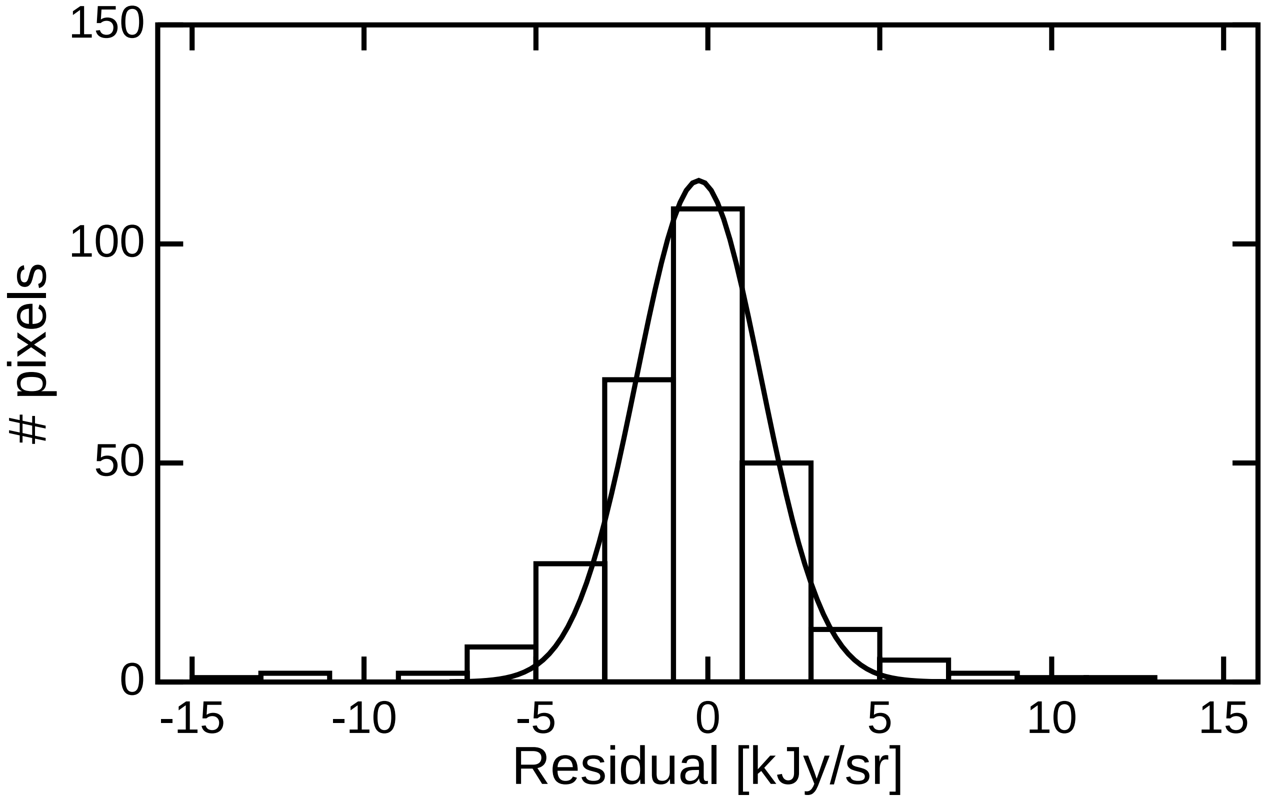

Fig. 5.— Histogram of $\mathrm{DZ}_i - B_i - \mathrm{DZ}(0)$ for the four dark spots combined at 2.2 μm. The solid Gaussian curve is fit to the highest three bins of the histogram.

Component	1.25 μm	2.20 μm
Scatter	1.49	0.51
Faint Source	0.34	0.18
Galaxies	0.05	0.10
Calibration	3.10	2.58
Zodiacal	5.87	3.79
Quadrature Sum	6.81	4.62

Table 2: Error budget for the CIRB.

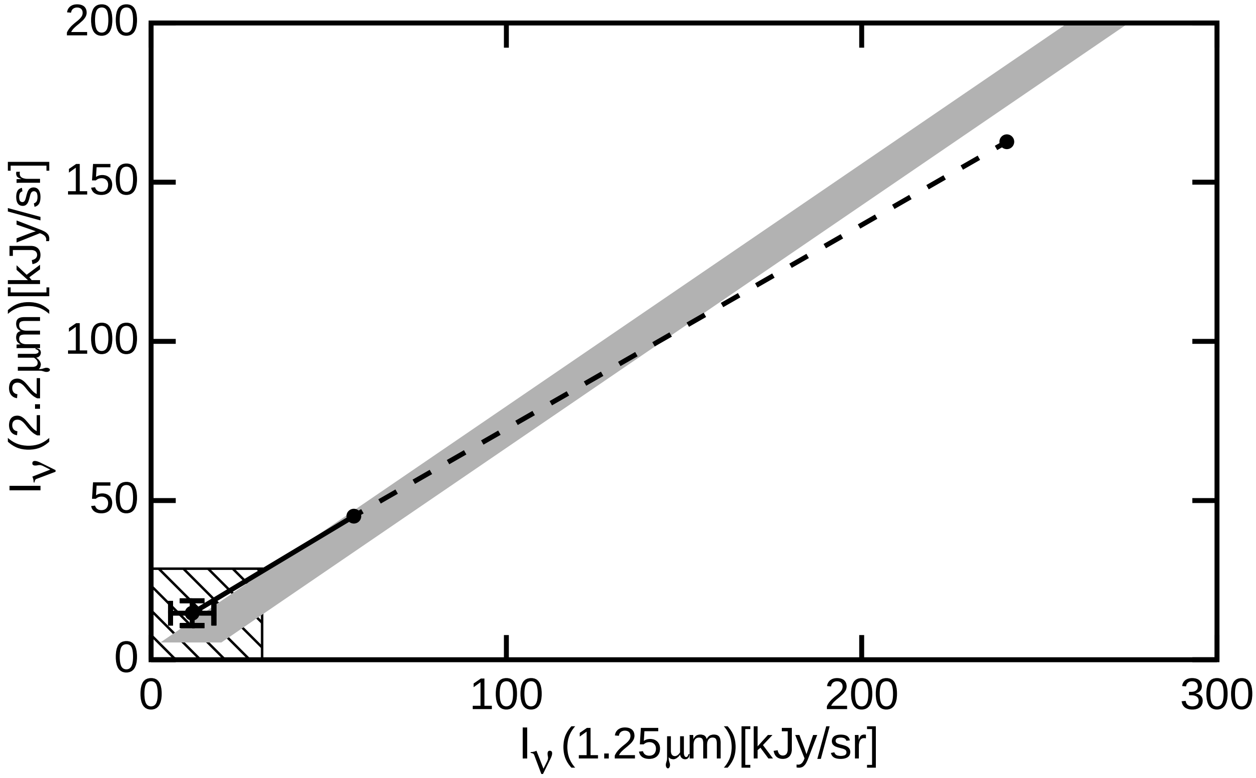

Fig. 6.— *J vs. K* intensities, averaged over the four dark spots, with the highest point showing the raw data, a dashed line showing the zodiacal model subtraction, and a solid line showing the star subtraction yielding the CIRB – the point with errorbars. The Hauser *et al.* (1998) upper limits are shown as the cross-hatched region, while the gray band shows the Dwek & Arendt (1998) correlation.

l [°]	b [°]	$\langle D_i \rangle$ [kJy/sr]	$\langle DZ_i \rangle$ [kJy/sr]	DZ(0) [kJy/sr]	F [kJy/sr]	CIRB [kJy/sr]
127.3	63.8	211.19	48.23	16.67	3.08	13.64
107.7	57.7	205.92	58.86	16.14	3.62	12.57
157.0	-82.7	314.80	51.48	10.59	2.94	7.70
257.8	-59.4	231.47	70.01	18.13	3.92	14.26

Table 3: Intensities of the 4 DIRBE dark spots at 1.25 μm.

Tests in three fields using deeper samples from the 2MASS catalog show that imposing the $K < 14$ cut on a $J < 14$ sample reduces the intensity by $< 0.3\%$. Table 3 gives the photometric quantities for the four dark fields at 1.25 μm. The $(10 \pm 10)\%$ correction of the faint star contribution derived from K-band star counts has been applied to F. Assuming a color of $J - K = 1$ for galaxies gives an estimate of 0.05 kJy sr^{-1} for the improperly subtracted faint galaxy contribution. This has been added to the CIRB estimates in the table. The mean of the CIRB estimates is 12.04 ± 1.49 kJy sr^{-1}, and this would change by ∓ 3.10 kJy sr^{-1} for $\pm 10\%$ changes in the flux of 1512 Jy for 0^{th} magnitude at 1.25 μm used in this paper. This value is the median of calibrations based on β And, α Tau, α Aur, α Boo, α Her, and β Peg. This calibration has an uncertainty of $\pm 2\%$ and differs from the Arendt *et al.* (1998) calibration by -2.4%. A $\pm 10\%$ uncertainty in the calibration of DIRBE *vs.* 2MASS has been adopted giving the error ± 3.10 kJy sr^{-1} listed in Table 2 . The systematic error due to interplanetary dust modeling is 5% of the ecliptic pole zodiacal intensity or ± 5.87 kJy sr^{-1}. Adding the errors in quadrature gives a result of 12.0 ± 6.8 kJy sr^{-1} or 28.9 ± 16.3 nW m^{-2} sr^{-1}. This is obviously not a significant detection due to the large uncertainty in the zodiacal foreground. However, a 2σ upper limit is $\nu I_\nu < 62$ nW m^{-2} sr^{-1} which is a slight improvement on Hauser *et al.* (1998).

The width of the combined histogram of the residuals for the J-band data is 2.32 kJy sr^{-1} or 5.6 nW m^{-2} sr^{-1} which gives an upper limit on extragalactic fluctuations since it also includes detector noise and star subtraction errors.

A CIRB of 12.0 ± 6.8 kJy sr^{-1} at 1.25 μm is fainter than the prediction of Dwek & Arendt (1998), whose correlation gives 23.5 ± 8.6 kJy sr^{-1} for this paper's K-band CIRB. Given the combined uncertainties in the difference, this is $< 1.2\sigma$ higher than the result in this paper.

5. Discussion

Subtracting the 2MASS catalog from the zodi-subtracted DIRBE data yields a statistically significant, isotropic background at 2.2 μm of 14.8 ± 4.6 kJy sr^{-1} which is consistent with the earlier results from Gorjian *et al.* (2000) (16.4 ± 4.4 kJy sr^{-1}) and Wright & Reese (2000) (16.9 ± 4.4 kJy sr^{-1}) within the systematic error associated with the modeling the zodiacal dust cloud. Averaging the results of Gorjian *et al.* (2000), Wright & Reese (2000) and this paper gives a CIRB at 2.2 μm of 16 ± 4 kJy sr^{-1}. This averaging has not reduced the estimated error which is dominated by systematic effects that affect all three results equally. The foreground due to interplanetary dust at 1.25 μm is too large to allow a CIRB detection, but an improved upper limit is found. Note that the Zodi-Subtracted Mission Average maps which used the Kelsall *et al.* (1998) zodiacal light model give a CIRB that is 13.75 kJy sr^{-1} larger at 1.25 μm and 6.08 kJy sr^{-1} larger at 2.2 μm than results obtained here using the zodiacal light model described in Wright (1998) and Gorjian *et al.* (2000) based on the very strong no-zodi principle of Wright (1997). Figure 6 shows a plot of the J-band intensity *vs.* K-band intensity averaged over the four dark spots analyzed in this paper. Three values are plotted: the average total intensity $\langle \mathrm{D} \rangle$, the average zodi-subtracted

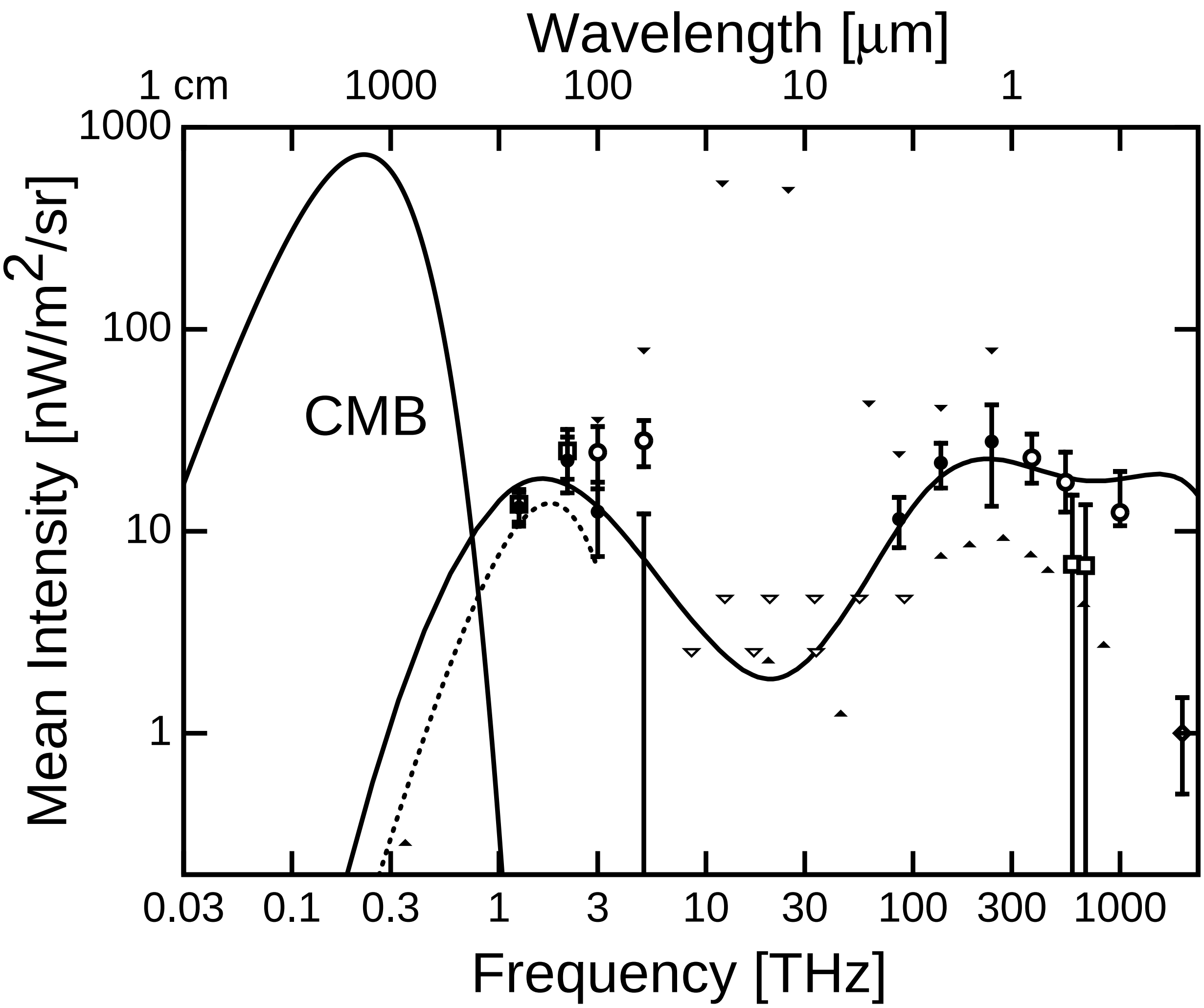

Fig. 7.— Comparison of CIRB values to previous determinations and upper limits. Lower limits from source counts from Smail *et al.* (1999) at 850 μm, Franceschini *et al.* (1997) at 15 & 6.7 μm, and Madau & Pozzetti (2000) at 2.2 to 0.3 μm. Solid upper limits from Hauser *et al.* (1998), open upper limit symbols using γ-rays from Funk *et al.* (1998) and Stanev & Franceschini (1998). Open squares at 240 & 140 μm from Hauser *et al.* (1998), open circles at 100 & 60 μm from Finkbeiner, Davis & Schlegel (2000), while the filled circle far IR data points are the Hauser *et al.* (1998) results modified by using this paper's zodiacal model. Dashed curve is from Fixsen *et al.* (1998). Filled circles from 3.5 to 1.25 μm are an average of Gorjian *et al.* (2000), Wright & Reese (2000) and this paper. Open circles from 0.8 to 0.3 μm are from Bernstein (1999). Open squares are from Dube, Wicks & Wilkinson (1977) and Toller (1983). The open diamond at 0.15 μm is from Hurwitz, Bowyer & Martin (1991).

intensity $\langle\mathrm{DZ}\rangle$, and the CIRB estimates. The Hauser *et al.* (1998) upper limits on the CIRB, the Dwek & Arendt (1998) correlation and the 1σ error bars from this paper are shown as well. This figure emphasizes the large subtractions that are involved in determining the CIRB from data taken 1 AU from the Sun: the zodiacal light is about 16 times larger than the CIRB at 1.25 μm and 8 times larger than the CIRB at 2.2 μm. Galactic stars are a problem in the large DIRBE beam, but in the selected dark spots the effect of stars is 4 times less than that of the zodiacal light.

Bernstein (1999) has measured the optical extragalactic background light and obtained results at $\lambda = 0.8,\ 0.55,\ \&\ 0.3\ \mu$m which are consistent with a reasonable extrapolation through the uncertain J-band result found here, as shown in Figure 7. Both Bernstein (1999) and this work face challenging and uncertain corrections for the zodiacal light, but the two papers use very different techniques and should not have systematic errors in common. Thus the lack of a discontinuity in the spectrum between 0.8 and 1.25 μm is an indication in favor of the background level reported here. The model shown in Figure 7 is the ΛCDM-Salpeter model from Primack *et al.* (1999) which appears to fit the observed far IR to near IR to optical ratios. But the model was multiplied by 1.84 to match the level of the observed background.

The *COBE* datasets were developed by the NASA Goddard Space Flight Center under the guidance of the COBE Science Working Group and were provided by the NSSDC. This publication makes use of data products from the Two Micron All Sky Survey, which is a joint project of the University of Massachusetts and the Infrared Processing and Analysis Center, funded by the National Aeronautics and Space Administration and the National Science Foundation.

REFERENCES

Arendt, R. *et al.* 1998, ApJ, 508, 74

Bernstein, R. 1999, in 'The Hy-Redshift Universe: Galaxy Formation and Evolution at High Redshift', eds. A. J. Bunker and W. J. M. van Breugel, ASP Conference Proceedings Vol. 193, 487

Boggess, N. W. *et al.* 1992, ApJ, 397, 420

Cutri, R. *et al.*, 2000, "Explanatory Supplement to the 2MASS Second Incremental Data Release," http://www.ipac.caltech.edu/2mass/releases/second/doc/explsup.html, viewed 28 March 2000.

Dwek, E. & Arendt, R. 1998, ApJ, 508, L9

Dube, R. R., Wicks, W. C. & Wilkinson, D. T. 1977, ApJ, 215, L51

Finkbeiner, D, Davis, M. & Schlegel, D. 2000, ApJ, 544, 81

Fixsen, D., Dwek, E., Mather, J. Bennett, C. & Shafer, R. 1998, ApJ, 508, 123

Franceschini, A. *et al.* 1997, "Source Counts and Background Radiation", in The Far Infrared and Submillimetre Universe, 159

Funk, B., Magnussen, N., Meyer, H., Rhode, W., Westerhoff, S. & Wiebel-Sooth, B. 1998, Astroparticle Physics, 9, 97

Gardner, J. P., Cowie, L. L. & Wainscoat, R. J. 1993, ApJ, 415, L9

Gorjian, V., Wright, E. & Chary, R. 2000, ApJ, 536, 550

Hauser, M. *et al.* 1998, ApJ, 508, 25

Hurwitz, M., Bowyer, S. & Martin, C. 1991, ApJ, 372, 167

Kashlinsky, A. & Odenwald, S. 2000, ApJ, 528, 74

Kelsall, T. *et al.* 1998, ApJ, 508, 44

Madau, P. & Pozzetti, L. 2000, MNRAS, 312, L9

Primack, J., Bullock, J., Somerville, R. & MacMinn, D. 1999, Astroparticle Physics, 11, 93

Smail, I., Ivison, R., Blain, A. & Kneib, J. 1999, "After the Dark Ages: When Galaxies were Young (the Universe at $2 < z < 5$)". 9th Annual October Astrophysics Conference in Maryland held 12-14 October, 1998. College Park, Maryland. Edited by S. Holt and E. Smith. American Institute of Physics Press, 1999, p. 312

Stanev, T. & Franceschini, A. 1998, ApJ, 494, L159

Toller, G. 1983, ApJ, 266, L79

Wainscoat, R., Cohen, M., Volk, K., Walker, H., & Schwartz, D. 1992, ApJS, 83, 111

Wright, E. 1997, BAAS, 29, 1354

Wright, E. 1998, ApJ, 496, 1

Wright, E. & Reese, E. 2000, ApJ, 545, 43

Wright, E. 2001, in preparation

This preprint was prepared with the AAS LaTeX macros v5.0.